Frontiers in Heat and Mass Transfer (FHMT), 16, 5 (2021)
DOI: 10.5098/hmt.16.5

Global Digital Central
ISSN: 2151-8629

Frontiers in Heat and Mass Transfer

Available at www.ThermalFluidsCentral.org

NUMERICAL APPROACH OF HEAT AND MASS TRANSFER OF MHD CASSON FLUID UNDER RADIATION OVER AN EXPONENTIALLY PERMEABLE STRETCHING SHEET WITH CHEMICAL REACTION AND HALL EFFECT

G. R. Ganesh and W. Sridhar*

Department of Mathematics,
Koneru Lakshmaiah Education Foundation,
Vaddeswaram, Guntur, A.P., 522502, India

ABSTRACT

In this paper, heat and mass transfer of MHD Casson fluid under radiation over an exponentially permeable stretching sheet with chemical reaction and Hall Effect investigated numerically. Suitable similarity transformations are used to convert the governing partial differential equations to nonlinear ordinary differential equations. Using a numerical technique named Keller box method the equations are then solved. Study of various effects such as chemical reaction, hall effect, suction /injection on magneto hydrodynamic Casson fluid along with radiation the heat source parameter, chemical reaction parameter, Schmidt number are tabulated for various parameters. Also local parameters are calculated and compared with previous literature the results are found to be in good agreement. The velocity, temperature, concentration visual representations are plotted for various parameters using matlab. Skin friction coefficient, Nusselt number and Sherwood number are calculated in both cases of Newtonian and non-Newtonian it is observed that the friction factor and the heat and mass transfer rates reduces for increase in magnetic parameter. Also for progressive values of radiation parameter, thermal grashof number, concentration grashof number and hall parameter, skin friction coefficient, heat and mass transfer rates increases where as they decreases for chemical reaction parameter, Schmidt number.

Keywords: MHD, Casson fluid, Chemical reaction, radiation, Hall Effect.

1. INTRODUCTION

Experience shows that due to several industrial applications of Non Newtonian fluids such as polymer industry and mining industry attracted many researchers to study about non Newtonian fluids. Also fluid flow over a stretching sheet is extensively used in manufacturing process because there is an association between stretching sheet and fluid that flows on it.

Dutta *et.al.* (1985) analyzed fluid flow on a stretching sheet with uniform heat flux and observed that with increase in Prandtl number first wall temperature increases quickly and then decreases gradually. Masahide and Tadashi (1988) proved that with the non-Newtonian property of blood, flow speed decreases along the stenosis. James and Milivoje (1990a) provided theoretical and practical study of heat transfer effects in both the cases of Newtonian and Non Newtonian fluid. Lai (1990b) derived a closed form of solutions for a special case of Lewis number. Lin and Wu (1995) studied boundary layer flow in case of a vertical plate and the effects of buoyancy ratio and Lewis number on Heat and mass transfer are observed. Magyari and Keller (1999) observed that boundary layer thickness increases on enhancing the value of wall temperature distribution by fixing Prandtl number also by keeping wall temperature fixed and enhancing Prandtl number. Swathi Mukhopadhyay *et al.* (2005) observed that by expanding the length of the stretching sheet velocity of the fluid decreases by reducing thickness of the fluid. Later, Subhas *et al*. (2010) analyzed non Newtonian fluid flow through a porous medium along with the effect of suction concluded that wall temperature will be decreased with the effect of viscous dissipation. Vedavathi *et.al* (2015) used Runge-Kutta fourth order and concluded that suction effect maintains fixed growth of the thermal, concentration, hydrodynamic boundary layers. After that Vedavathi *et.al* (2017) concluded that on increasing radiation absorption parameter velocity profiles will be enhanced and increasing Prandtl number skin friction number decreases.

Talla, Kumari and Sridhar (2018a) studied MHD Casson fluid flow over a exponentially stretching surface and observed that with increase in Casson parameter velocity reduces and concentration increases. Reddy and Krishna (2018b) observed that as the Soret number increases velocity boundary layer, thermal boundary layer, concentration boundary layer diminishes. Chandra Sekhar (2018c) observed that temperature increases with increase of chemical reaction parameter. Konda Reddy *et al.* (2018d) studied MHD mixed convection flow of a Casson Nano fluid over a nonlinear stretching sheet temperature, concentration enhanced and velocity diminished with increase in Casson parameter. Charan Kumar *et al.* (2018e) used RK- Fehlberg method to study the effects of joule heating and chemical reaction effects on fluid flow over a stretching sheet along with radiation and porous medium. Anki Reddy and Suneetha (2018f) concluded that temperature of the fluid and thermal relaxation time are oppositely related. Ghiasi and Saleh (2018g) witnessed that casson fluid along with suction effect reduces heat, mass transfer rates. Flilihi *et al.* (2019a) concluded that fluid temperature raises with increase in dissipation parameter. Dharmaiah *et al.* (2019b) used perturbation method and observed that chemical reaction parameter dominates the concentration profiles. Sampath and Pai (2019c) found that enhancing magnetic parameter skin friction decreases. Nagaraju *et al.*(2019d) used HAM technique and concluded that raise in magnetic parameter enhances velocity also energy dissipation step ups causing increase in temperature, later Huang pin *et al.*(2019e) used Keller box method and observed that suction increases the Nusselt number and Sherwood number. Blowing reduces them. Ganapathirao *et al.* (2019f) found that skin friction and coefficient of heat transfer raises with enhancing buoyancy parameter. Ibrahim *et al.* (2019g) observed that velocity increases with increasing buoyancy parameter. Raghunandana Sai and Ramana Murthy (2019h) studied the impact of various parameters on velocity and temperature profiles and observed that with increase in Prandtl number and time temperature increases. Ravi Kumar *et al.* (2019i) noticed that with

*Corresponding Author Email: sridharwuriti@gmail.com

increase in slip parameter, Grashof's number velocity increases. Kavitha and Naikoti (2019j) used quasi-linearization technique to study the power law fluid flow under the influence of radiation. Swamy *et al.* (2019k) studied MHD flow in a porous channel with suction and observed that as the intensity of the magnetic field increases fluid velocity reduces. Vijaya and Reddy (2019l) analyzed the MHD Casson fluid flow on a vertical porous plate using Perturbation technique method. Manjula and Chandra Sekhar (2019m) observed Soret and heat generation effects on Casson fluid flow concluded that raise in Soret number values increases buoyancy force hence velocity increases. Sivaiah *et al.* (2019n) concluded that due to thermal radiation parameter, temperature decreases and with the presence of Eckert number temperature increases. Dharmaiah. *et al.* (2019o) implemented perturbation technique and noticed that concentration of the fluid reduces with the presence of chemical reaction. Balamurugan *et al.* (2020a) concluded that entropy generation increases for higher values of magnetic parameter or thermal radiation parameter. Later Vijaya *et al.* (2020b) used bvp4c technique and noted that for increasing values of magnetic parameter velocity of fluid improved. Dharmaiah. *et al.* (2020c) studied the influence of hall and ion slip on a Nano fluid and concluded that skin friction coefficient raises with magnetic parameter.Nagalaksmi and vijaya(2020d) used Runge Kutta method and observes for progressive values of Prandtl number thermal boundary layer thickness diminishes. Ibrahim.*et al.* (2020e) used Homotopy analysis method to study the influence of various parameters like radiation, chemical reaction of MHD casson fluid flow over a stretching sheet.

The study of flow above an exponentially stretching sheet has significant applications in various industries and technological processes for example fluid film condensation process, cooling process of metallic sheets, design of chemical processing equipment, polymer industries. Also the radiation effect on MHD boundary layer flow has various applications in manufacturing industries like glass-fiber production, paper production etc. Hall effect has some industrial applications like automotive safety, fluid monitoring, building automation, personal electronics like disk drives, power supply protectors .with this interest in the present paper, Keller Box method was implemented to study the influence of hall effect in presence of radiation and chemical reaction of MHD Casson fluid flow on an exponentially permeable stretching sheet.

2. FORMULATION OF THE PROBLEM

In this study a steady, two dimensional, incompressible, radiative, MHD Casson fluid flow over an exponentially permeable stretching sheet under the influence of Hall Effect is considered. u, v represents velocity components in x and y directions. The exponentially stretching sheet is assumed to be at y=0. Also flow is assumed to be above x-axis only. Magnetic field is applied externally normal to stretching sheet. The magnetic Reynolds number is very small because of the magnetic field. Here we used external heat source, Hall Effect, chemical reaction.

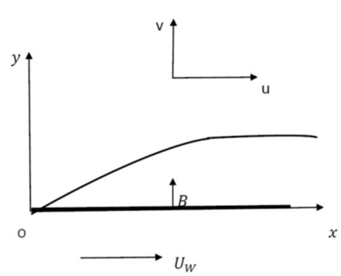

Fig. 1 Flow model of the problem

The rheological equation of Casson fluid is

$$\tau_{ij} = \begin{cases} 2\left(\mu_B + p_y * (2\pi)^{-0.5}\right)e_{ij}, \pi > \pi_c \\ 2\left(\mu_B + p_y * (2\pi_c)^{-0.5}\right)e_{ij}, \pi < \pi_c \end{cases}$$

Where μ_B is plastic dynamic viscosity, P_y is yield stress, π is (i, j) th component of deformation rate, π_c is critical value of this product.

Supporting to the above assumptions the guiding partial differential equations are taken as below.

$$u_x + v_y = 0 \tag{1}$$

$$uu_x + vu_y = \upsilon(1+\frac{1}{\beta})u_{xx} + g\beta_T(T-T_\infty) + g\beta_C(C-C_\infty) - \frac{\sigma B^2 u}{\rho(1+m^2)} \tag{2}$$

$$uT_x + vT_y = \frac{k}{\rho C_p}T_{yy} + \frac{\upsilon}{C_p}(1+\frac{1}{\beta})u_y^2 - \frac{1}{\rho C_p}Q_0(T-T_\infty) + \frac{\sigma B^2 u^2}{\rho(1+m^2)} - \frac{1}{\rho C_p}(q_r)_y \tag{3}$$

$$uC_x + vC_y = D_m C_{yy} - k_1(C - C_\infty) \tag{4}$$

Boundary conditions are

$$\left.\begin{array}{lll} u = U, & & u \to 0, \\ v = -V(x), \text{ at } y = 0 \;\& & T \to T_\infty, & \text{as } y \to \infty \\ T = T_w, & C \to C_\infty & \\ C = C_w & & \end{array}\right\} \tag{5}$$

By observing the equations here we introduce the similarity transformations,

$$\left.\begin{array}{l} u = U_0 e^{\frac{Nx}{L}} f'(\eta) \\ v = -\sqrt{\dfrac{U_0\upsilon}{2L}} e^{\frac{Nx}{2L}} N\left(f(\eta) + \eta f'(\eta)\right) \\ \psi = \sqrt{2U_0\upsilon L}\, e^{\frac{Nx}{2L}} f(\eta) \\ T = T_\infty + T_0 e^{\frac{2Nx}{L}} \theta(\eta) \\ C = C_\infty + C_0 e^{\frac{2Nx}{L}} \phi(\eta) \\ \eta = y\sqrt{\dfrac{U_0}{2\upsilon L}} e^{\frac{Nx}{2L}} \end{array}\right\} \tag{6}$$

The partial differential equations are transformed to

$$\left(1+\frac{1}{\beta}\right)\frac{d^3 f}{d\eta^3} + N\left[f\frac{d^2 f}{d\eta^2} - 2\left(\frac{df}{d\eta}\right)^2\right] + 2Gr\,\theta + 2Gc\,\phi - \frac{Ha^2}{1+m^2}\frac{df}{d\eta} = 0 \tag{7}$$

$$\left(1+\frac{4}{3}R\right)\frac{d^2\theta}{d\eta^2} + \Pr\ N\left[f\frac{d\theta}{d\eta} - 4\frac{df}{d\eta}\theta\right] + \left(1+\frac{1}{\beta}\right)\Pr\ Ec\frac{d^2 f}{d\eta^2} - \Pr\ Q\,\theta + \frac{\Pr\ J}{1+m^2}\frac{d^2 f}{d\eta^2} = 0 \tag{8}$$

$$\frac{d^2\phi}{d\eta^2} + Sc\left[f\frac{d\phi}{d\eta} - 4\frac{df}{d\eta}\phi\right] - Sc\,\gamma\phi = 0 \tag{9}$$

DOI: 10.5098/hmt.16.5
ISSN: 2151-8629

Boundary conditions transformed to

$$\left.\begin{aligned} &f = S\,,\ f' = 1 && \text{at } \eta = 0 \\ &\theta = 1\,,\ \phi = 1 && \\ &f' = 0 && \text{at } \eta \to \infty \\ &\theta = 0\,,\ \phi = 0 && \end{aligned}\right\} \tag{10}$$

3. NUMERICAL PROCEDURE

The moderate implicit finite difference method called Keller Box method to convert equations (7)-(9) into first order. By using this method, the resultant equations are linearized and then converted into matrix form by introducing Newton's method. Finally, the tri-diagonal elimination method is applied to solve the linear system of equations Cebeci *et al.* (1988).

Introducing

$$\begin{aligned} &f' = p\,,\ p' = q \\ &g = \theta\,,\ g' = t \\ &s = \phi\,,\ s' = n \end{aligned} \tag{11}$$

The equations (7), (8), (9) are transformed to

$$\left(1+\frac{1}{\beta}\right)q' + N\left[fq - 2p^2\right] + 2Grg + 2Gcs - \frac{Ha^2}{1+m^2}p = 0 \tag{12}$$

$$\left(1+\frac{4R}{3}\right)t' + \Pr N\left[ft - 4pg\right] + \left(1+\frac{1}{\beta}\right)\Pr Ecq^2 - \Pr Qg + \frac{\Pr J}{1+m^2}p^2 = 0 \tag{13}$$

$$n' + Sc\left[fn - 4ps\right] - Sc\,\gamma s = 0 \tag{14}$$

Using finite differences

$$f_j - f_{j-1} = h_j\left(\frac{p_j + p_{j-1}}{2}\right)$$

$$p_j - p_{j-1} = h_j\left(\frac{q_j + q_{j-1}}{2}\right)$$

$$g_j - g_{j-1} = h_j\left(\frac{t_j + t_{j-1}}{2}\right)$$

$$s_j - s_{j-1} = h_j\left(\frac{n_j + n_{j-1}}{2}\right)$$

$$\left(1+\frac{1}{\beta}\right)\left(\frac{q_j - q_{j-1}}{h_j}\right) + N\left[\left(\frac{f_j+f_{j-1}}{2}\right)\left(\frac{q_j+q_{j-1}}{2}\right) - 2\left(\frac{p_j+p_{j-1}}{2}\right)^2\right] + 2Gr\left(\frac{g_j+g_{j-1}}{2}\right) + 2Gc\left(\frac{s_j+s_{j-1}}{2}\right) - \frac{Ha^2}{1+m^2}\left(\frac{p_j+p_{j-1}}{2}\right) = 0 \tag{15}$$

$$\left(1+\frac{4R}{3}\right)\left(\frac{t_j - t_{j-1}}{h_j}\right) + \Pr N\left[\left(\frac{f_j+f_{j-1}}{2}\right)\left(\frac{t_j+t_{j-1}}{2}\right) - 4\left(\frac{p_j+p_{j-1}}{2}\right)\left(\frac{g_j+g_{j-1}}{2}\right)\right] + \left(1+\frac{1}{\beta}\right)\Pr Ec\left(\frac{q_j+q_{j-1}}{2}\right)^2 - \Pr Q\left(\frac{g_j+g_{j-1}}{2}\right) + \frac{\Pr J}{1+m^2}\left(\frac{p_j+p_{j-1}}{2}\right)^2 = 0$$

$$\left(\frac{n_j + n_{j-1}}{h_j}\right) + Sc\left[\left(\frac{f_j+f_{j-1}}{2}\right)\left(\frac{n_j+n_{j-1}}{2}\right) - 4\left(\frac{p_j+p_{j-1}}{2}\right)\left(\frac{s_j+s_{j-1}}{2}\right)\right] - Sc\,\gamma\left(\frac{s_j+s_{j-1}}{2}\right) = 0$$

We linearize the system of equations given in (15) Using Newton's method for that we introduce

$$\begin{aligned} f_j^{k+1} &= f_j^k + \delta f_j^k \\ p_j^{k+1} &= p_j^k + \delta p_j^k \\ q_j^{k+1} &= q_j^k + \delta q_j^k \\ g_j^{k+1} &= g_j^k + \delta g_j^k \\ t_j^{k+1} &= t_j^k + \delta t_j^k \\ s_j^{k+1} &= s_j^k + \delta s_j^k \\ n_j^{k+1} &= n_j^k + \delta n_j^k \end{aligned} \tag{16}$$

Substitute them in above system (15) we get the system of equations as

$$\begin{aligned} &\delta f_j - \delta f_{j-1} - \frac{h_j}{2}\left(\delta p_j + \delta p_{j-1}\right) = (r_1)_j \\ &\delta p_j - \delta p_{j-1} - \frac{h_j}{2}\left(\delta q_j + \delta q_{j-1}\right) = (r_2)_j \\ &\delta g_j - \delta g_{j-1} - \frac{h_j}{2}\left(\delta t_j + \delta t_{j-1}\right) = (r_3)_j \\ &\delta s_j - \delta s_{j-1} - \frac{h_j}{2}\left(\delta n_j + \delta n_{j-1}\right) = (r_4)_j \\ &(a_1)_j\delta q_j + (a_2)_j\delta q_{j-1} + (a_3)_j\delta f_j + (a_4)_j\delta f_{j-1} \\ &+ (a_5)_j\delta p_j + (a_6)_j\delta p_{j-1} + (a_7)_j\delta g_j + (a_8)_j\delta g_{j-1} \\ &+ (a_9)_j\delta s_j + (a_{10})_j\delta s_{j-1} = (r_5)_j \\ &(b_1)_j\delta t_j + (b_2)_j\delta t_{j-1} + (b_3)_j\delta f_j + (b_4)_j\delta f_{j-1} + (b_5)_j\delta g_j + \\ &(b_6)_j\delta g_{j-1} + (b_7)_j\delta q_j + (b_8)_j\delta q_{j-1} = (r_6)_j \\ &(c_1)_j\delta n_j + (c_2)_j\delta n_{j-1} + (c_3)_j\delta f_j + (c_4)_j\delta f_{j-1} + (c_5)_j\delta s_j \\ &+ (c_6)_j\delta s_{j-1} + (c_7)_j\delta p_j + (c_8)_j\delta p_{j-1} = (r_7)_j \end{aligned} \tag{17}$$

Where j=1, 2, 3

$$\begin{aligned} (r_1)_j &= f_{j-1} - f_j + \frac{h_j}{2}\left(p_j + p_{j-1}\right) \\ (r_2)_j &= p_{j-1} - p_j + \frac{h_j}{2}\left(q_j + q_{j-1}\right) \\ (r_3)_j &= g_{j-1} - g_j + \frac{h_j}{2}\left(t_j + t_{j-1}\right) \\ (r_4)_j &= s_{j-1} - s_j + \frac{h_j}{2}\left(n_j + n_{j-1}\right) \end{aligned} \tag{18}$$

DOI: 10.5098/hmt.16.5 ISSN: 2151-8629

$$(r_5)_j = q_{j-1} - q_j - \frac{N\beta h_j}{4(\beta+1)}(f_j + f_{j-1})(q_j + q_{j-1}) + \frac{N\beta h_j}{2(\beta+1)}(p_j + p_{j-1})^2 - \frac{Gr\beta h_j}{\beta+1}(g_j + g_{j-1}) - \frac{Gc\beta h_j}{\beta+1}(s_j + s_{j-1}) + \frac{Ha^2\beta h_j}{2(\beta+1)(1+m^2)}(p_j + p_{j-1})$$

$$(r_6)_j = t_{j-1} - t_j - \frac{3\Pr N}{4(3+4R)}(f_j + f_{j-1})(t_j + t_{j-1}) + \frac{3\Pr N}{3+4R}(p_j + p_{j-1})(g_j + g_{j-1}) - \frac{\beta+1}{\beta}\frac{3\Pr Ech_j}{4(3+4R)}(q_j + q_{j-1})^2 + \frac{3\Pr Q}{2(3+4R)}(g_j + g_{j-1}) - \frac{3\Pr h_j J}{4(3+4R)(1+m^2)}(p_j + p_{j-1})^2$$

$$(r_7)_j = n_{j-1} - n_j - \frac{Sch_j}{4}(f_j + f_{j-1})(n_j + n_{j-1}) + Sch_j(p_j + p_{j-1})(s_j + s_{j-1}) + \frac{Sc\gamma h_j}{2}(s_j + s_{j-1})$$

$$(a_2)_j = (a_1)_j - 2.0$$
$$(a_3)_j = \frac{N\beta h_j}{4(\beta+1)}(q_j + q_{j-1})$$
$$(a_4)_j = (a_3)_j$$
$$(a_5)_j = -\frac{N\beta h_j}{\beta+1}(p_j + p_{j-1}) - \frac{Ha^2\beta h_j}{2(\beta+1)(1+m^2)}(p_j + p_{j-1})$$
$$(a_6)_j = (a_5)_j \tag{19}$$
$$(a_7)_j = \frac{Gr\beta h_j}{\beta+1},$$
$$(a_8)_j = (a_7)_j$$
$$(a_9)_j = \frac{Gc\beta h_j}{\beta+1},$$
$$(a_{10})_j = (a_9)_j$$
$$(b_1)_j = 1 + \frac{3\Pr Nh_j}{4(3+4R)}(f_j + f_{j-1})$$
$$(b_2)_j = (b_1)_j - 2.0$$
$$(b_3)_j = \frac{3\Pr Nh_j}{4(3+4R)}(t_j + t_{j-1}) \tag{20}$$
$$(b_4)_j = (b_3)_j$$
$$(b_5)_j = \frac{-3\Pr Nh_j}{3+4R}(p_j + p_{j-1}) - \frac{3\Pr Qh_j}{2(3+4R)}$$
$$(b_6)_j = (b_5)_j$$
$$(b_7)_j = -\frac{3\Pr Nh_j}{(3+4R)}(g_j + g_{j-1}) + \frac{3}{2}\frac{\Pr h_j J}{(3+4R)(1+m^2)}(p_j + p_{j-1})$$
$$(b_8)_j = (b_7)_j$$
$$(b_9)_j = \frac{3}{2}\left(\frac{\beta+1}{\beta}\right)\frac{\Pr Ech_j}{(3+4R)}(q_j + q_{j-1})$$
$$(b_{10})_j = (b_9)_j$$
$$(c_1)_j = 1 + \frac{Sch_j}{4}(f_j + f_{j-1})$$
$$(c_2)_j = (c_1)_j - 2.0$$
$$(c_3)_j = \frac{Sch_j}{4}(n_j + n_{j-1})$$
$$(c_4)_j = (c_3)_j \tag{21}$$
$$(c_5)_j = -Sch_j(p_j + p_{j-1}) - \frac{Sc\gamma h_j}{2}$$
$$(c_6)_j = (c_5)_j$$
$$(c_7)_j = -Sch_j(s_j + s_{j-1})$$
$$(c_8)_j = (c_7)_j$$

For j=1, 2, 3….
The system of equations become

$$[A_1][\delta_1] + [C_1][\delta_2] = [r_1] \tag{22}$$
$$[B_2][\delta_1] + [A_2][\delta_2] + [C_2][\delta_3] = [r_2]$$
…….
$$[B_{j-1}][\delta_1] + [A_{j-1}][\delta_2] + [C_{j-1}][\delta_3] = [r_{j-1}]$$
$$[B_j][\delta_{j-1}] + [A_j][\delta_j] = [r_j]$$

Where,

$$A_1 = \begin{bmatrix} 0 & 0 & 0 & 1 & 0 & 0 & 0 \\ d & 0 & 0 & 0 & d & 0 & 0 \\ 0 & d & 0 & 0 & 0 & d & 0 \\ 0 & 0 & -1 & 0 & 0 & 0 & d \\ (a_2)_1 & 0 & (a_{10})_1 & (a_3)_1 & (a_1)_1 & 0 & 0 \\ (b_{10})_1 & (b_2)_1 & 0 & (b_3)_1 & (b_9)_1 & (b_1)_1 & 0 \\ 0 & 0 & (c_6)_1 & (c_3)_1 & 0 & 0 & (c_1)_1 \end{bmatrix}$$

DOI: 10.5098/hmt.16.5
ISSN: 2151-8629

$$A_j = \begin{bmatrix} d & 0 & 0 & 1 & 0 & 0 & 0 \\ -1 & 0 & 0 & 0 & d & 0 & 0 \\ 0 & -1 & 0 & 0 & 0 & d & 0 \\ 0 & 0 & -1 & 0 & 0 & 0 & d \\ (a_6)_2 & (a_8)_2 & (a_{10})_2 & (a_3)_2 & (a_1)_2 & 0 & 0 \\ (b_8)_2 & (b_6)_2 & 0 & (b_3)_2 & (b_9)_2 & (b_1)_2 & 0 \\ (c_8)_2 & 0 & (c_6)_2 & (c_3)_2 & 0 & 0 & (c_1)_2 \end{bmatrix}$$

Where j= 2, 3, n-1

$$B_j = \begin{bmatrix} 0 & 0 & 0 & -1 & 0 & 0 & 0 \\ 0 & 0 & 0 & 0 & d & 0 & 0 \\ 0 & 0 & 0 & 0 & 0 & d & 0 \\ 0 & 0 & 0 & 0 & 0 & 0 & d \\ 0 & 0 & 0 & (a_4)_2 & (a_2)_2 & 0 & 0 \\ 0 & 0 & 0 & (b_4)_2 & (b_{10})_2 & (b_2)_2 & 0 \\ 0 & 0 & 0 & (c_4)_2 & 0 & 0 & (c_2)_2 \end{bmatrix} \text{ and}$$

$$C_j = \begin{bmatrix} d & 0 & 0 & 0 & 0 & 0 & 0 \\ 1 & 0 & 0 & 0 & 0 & 0 & 0 \\ 0 & 1 & 0 & 0 & 0 & 0 & 0 \\ 0 & 0 & 1 & 0 & 0 & 0 & 0 \\ (a_5)_2 & (a_7)_2 & (a_9)_2 & 0 & 0 & 0 & 0 \\ (b_7)_2 & (b_5)_2 & 0 & 0 & 0 & 0 & 0 \\ (c_7)_2 & 0 & (c_5)_2 & 0 & 0 & 0 & 0 \end{bmatrix}$$

Where j= 1, 2, 3, n-1.

The resultant linear equations are solved by LU decomposition method, the process of calculation should be terminated until it satisfies convergence criteria. The calculations are terminated for $\left|\delta g_0^{(i)}\right| < \varepsilon$ where $\varepsilon = 0.000001$.

4. RESULTS AND DISCUSSION

Graphs are plotted for various parameters like Hartman's number, exponential parameter, Thermal Grashof's number, concentration Grashof's number, radiation parameter, Prandtl number, heat source parameter, Eckert number, Schmidt number, chemical reaction parameter, Suction parameter, Hall parameter using MATLAB.

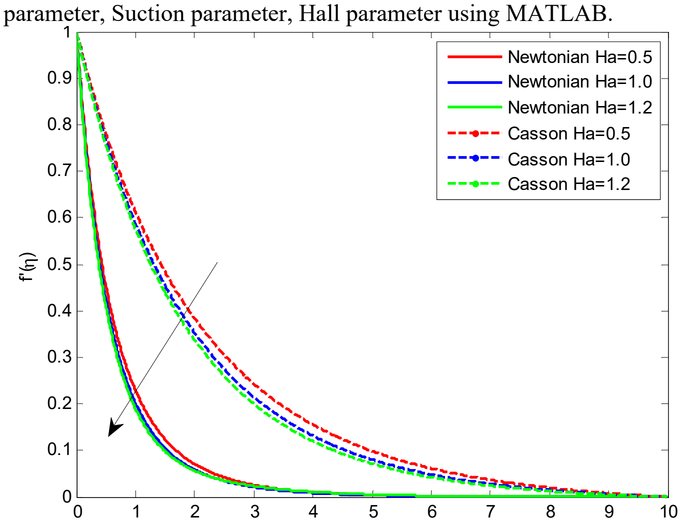

Fig. 2 Effect of Ha on Velocity

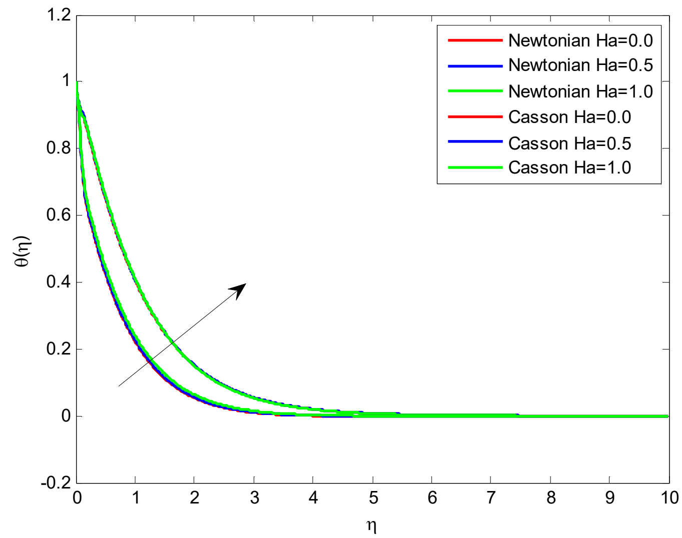

Fig. 3 Effect of Ha on Temperature

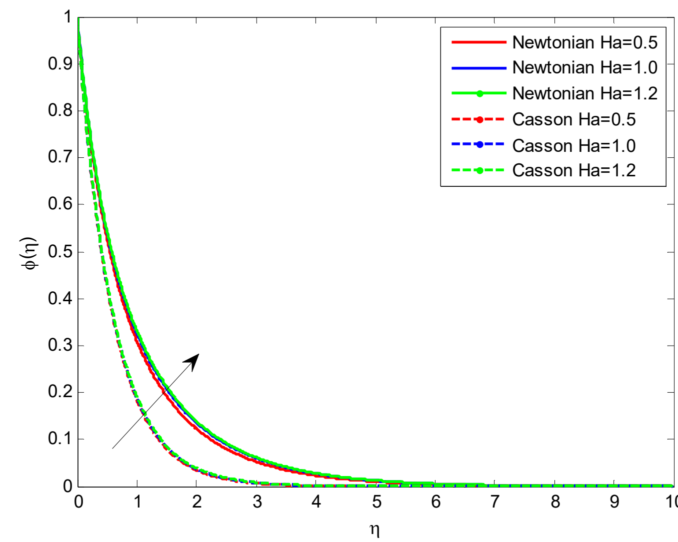

Fig. 4 Effect of Ha on concentration

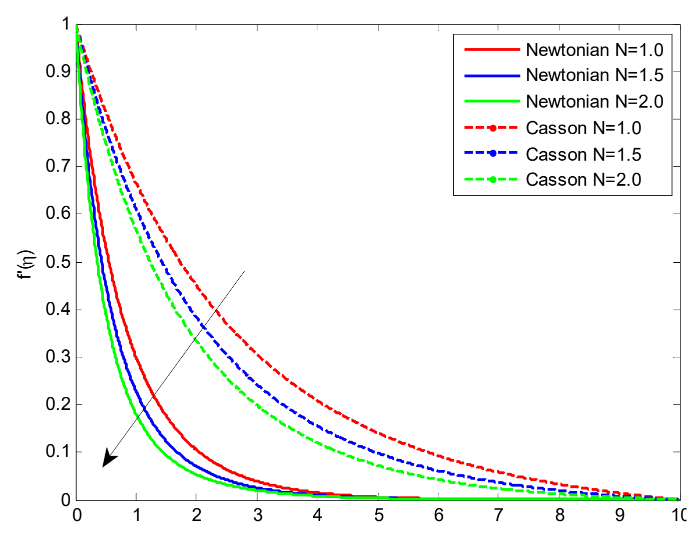

Fig. 5 Effect of N on Velocity

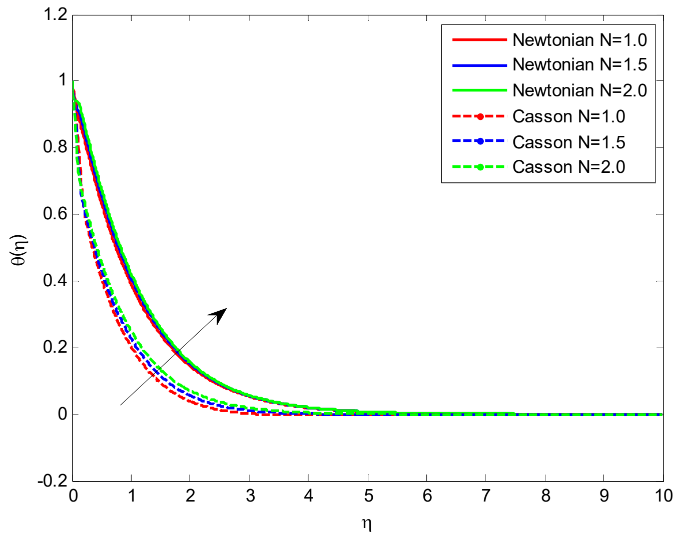

Fig. 6 Effect of N on Temperature

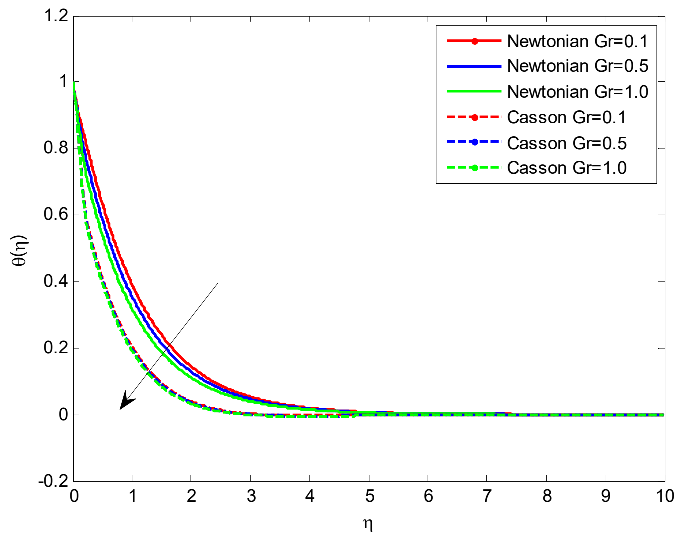

Fig. 9 Effect of Gr on temperature

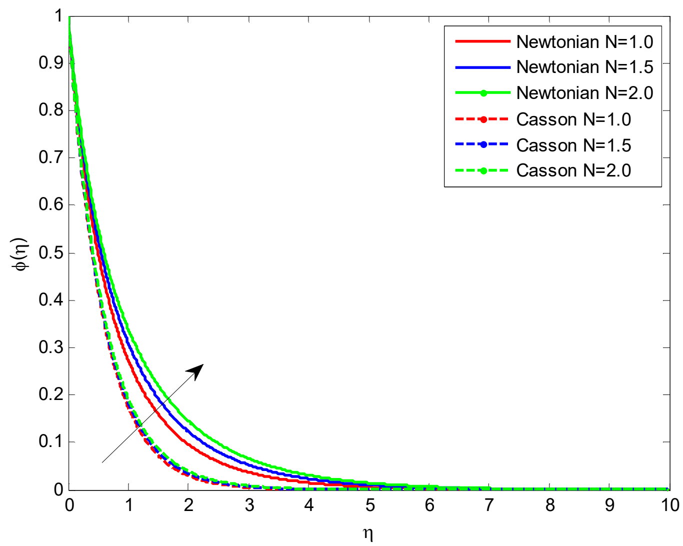

Fig. 7 Effect of N on Concentration

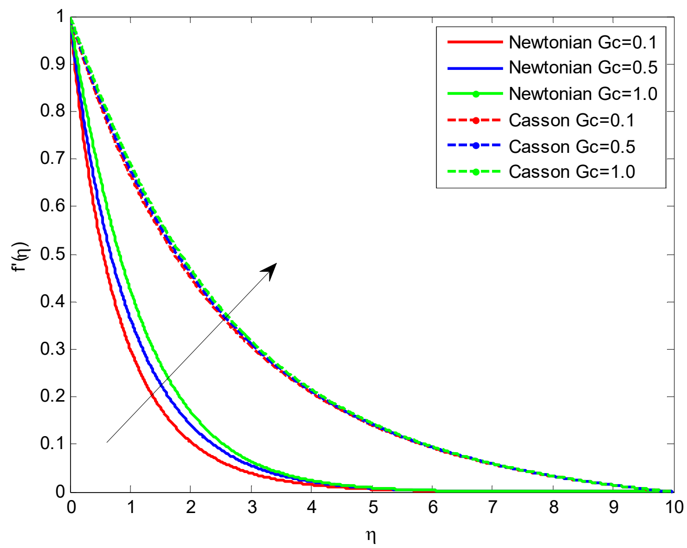

Fig. 10 Effect of Gc on velociy

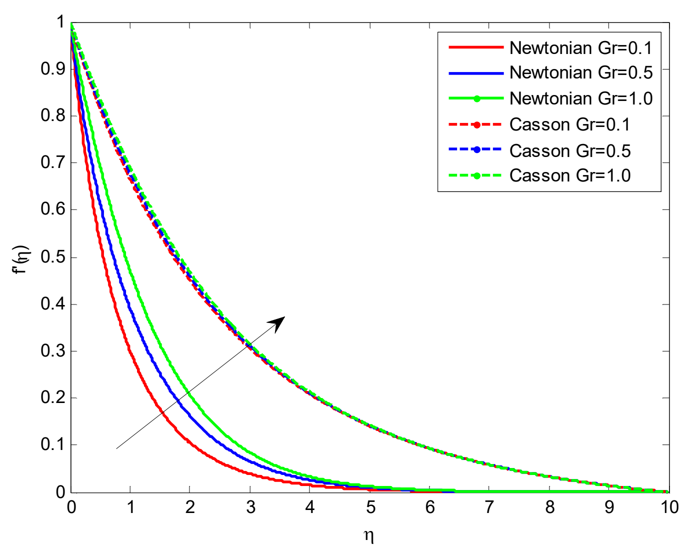

Fig. 8 Effect of Gr on Velocity

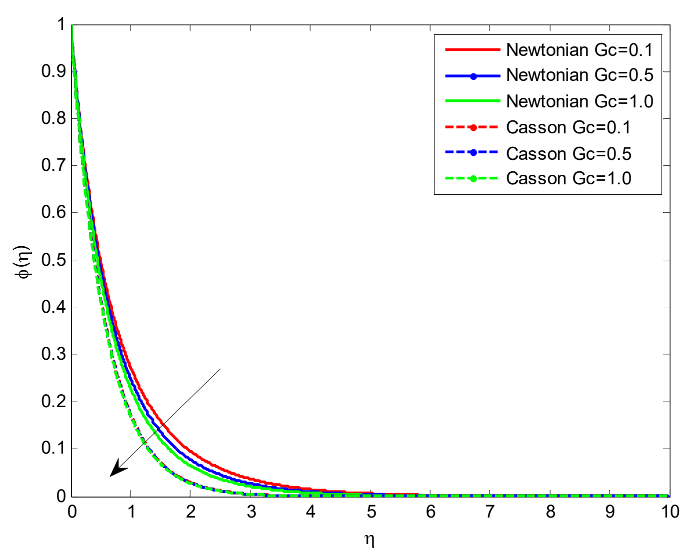

Fig. 11 Effect of Gc on Concentration

DOI: 10.5098/hmt.16.5
ISSN: 2151-8629

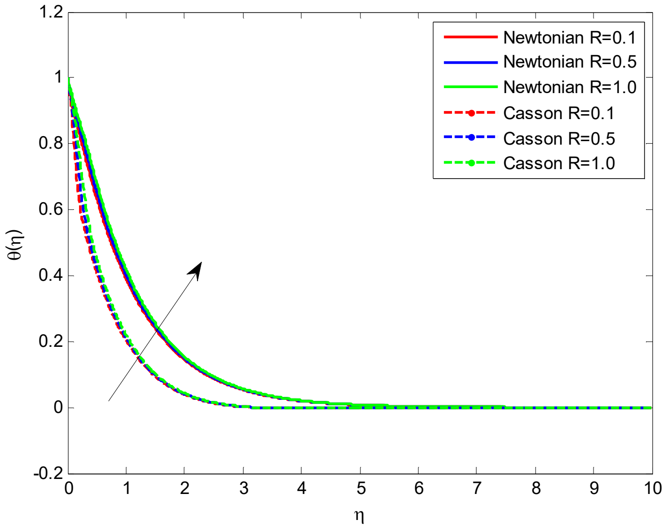

Fig. 12 Effect of R on temperature

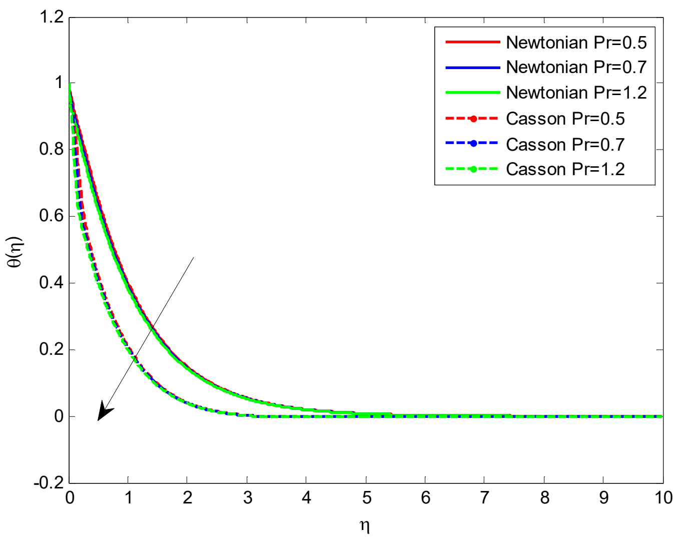

Fig. 13 Effect of Pr on Temperature

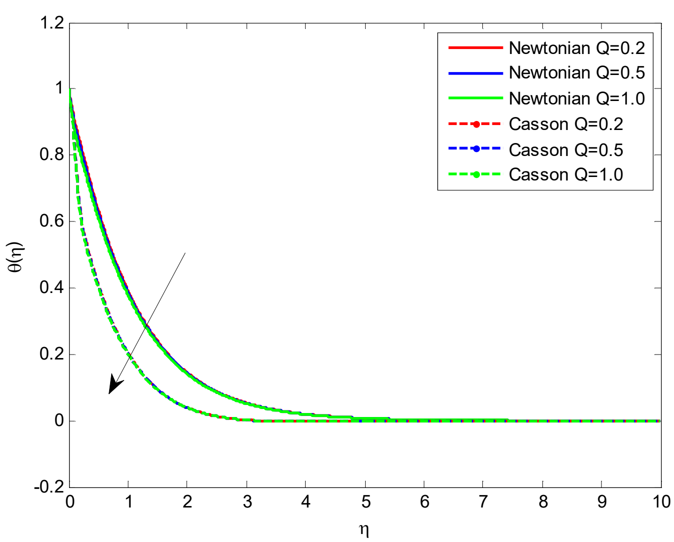

Fig. 14 Effect of Q on temperature

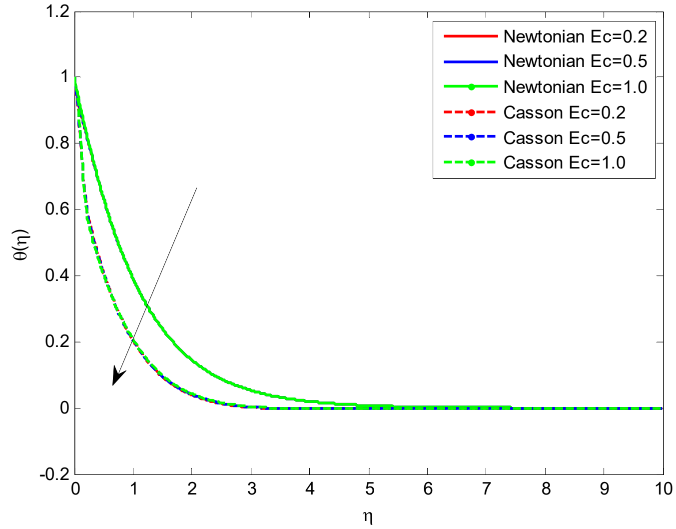

Fig. 15 Effect of Ec on Temperature

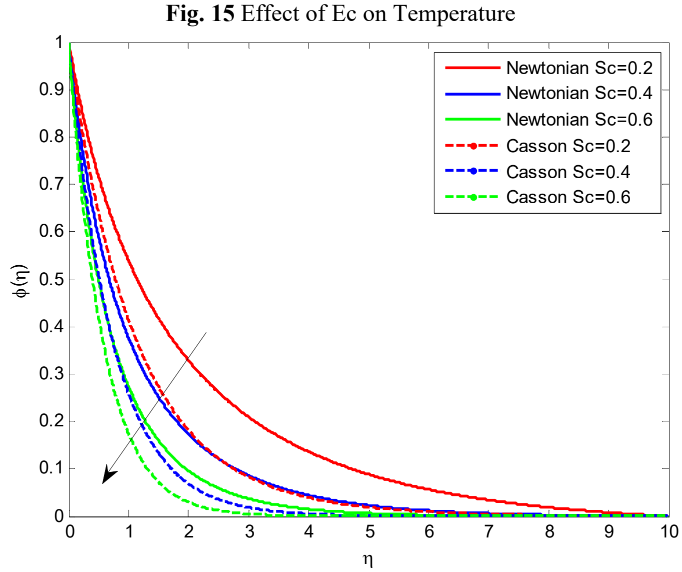

Fig. 16 Effect of Sc on concentration

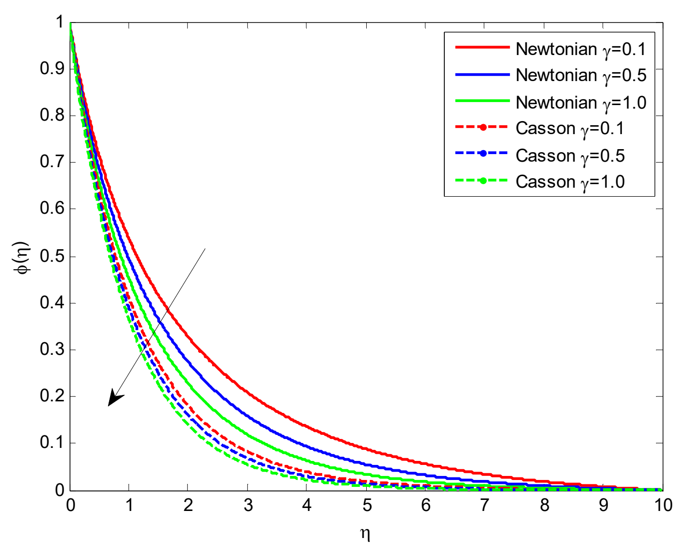

Fig. 17 Effect of γ on concentration

DOI: 10.5098/hmt.16.5
ISSN: 2151-8629

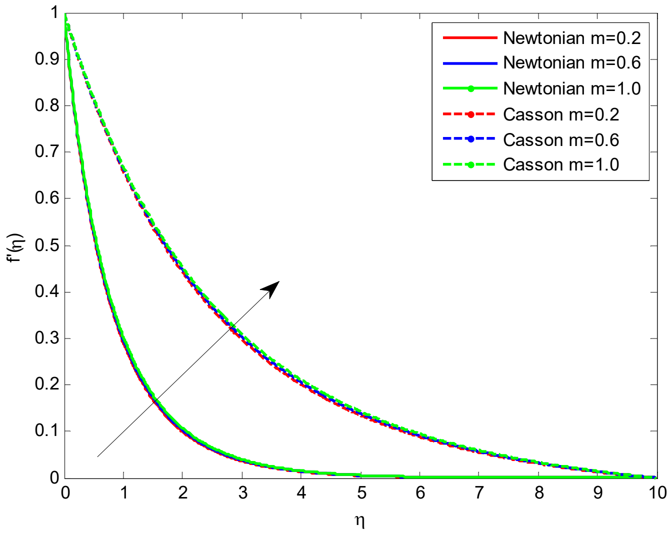

Fig. 18 Effect of m on velocity

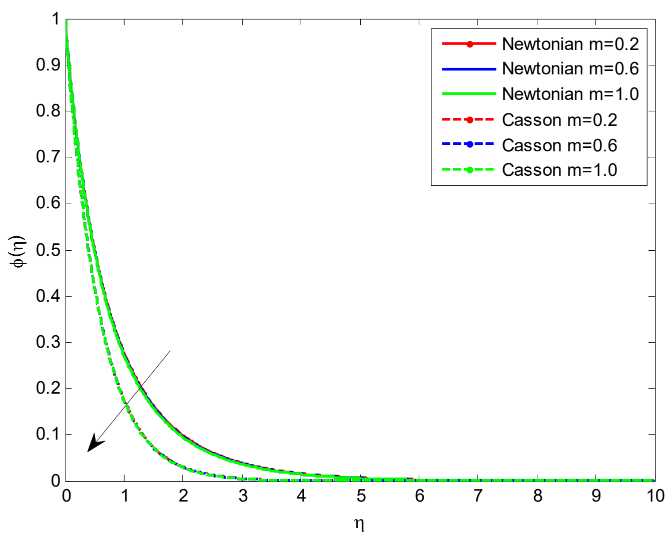

Fig. 19 Effect of m on Concentration

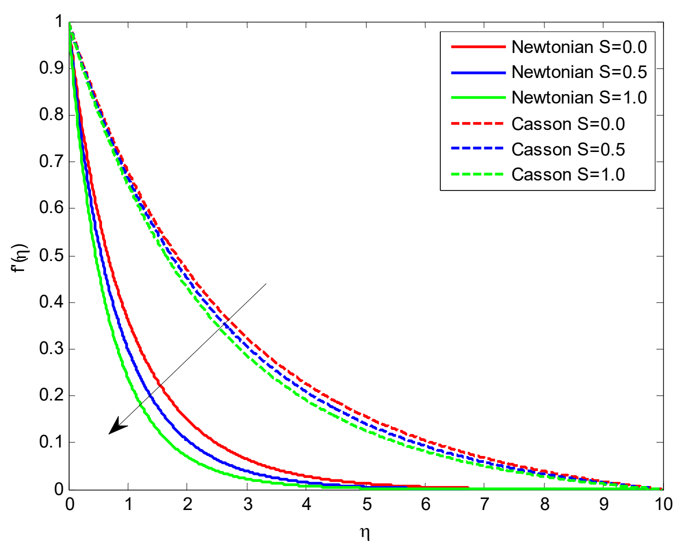

Fig. 20 Effect of S on velocity

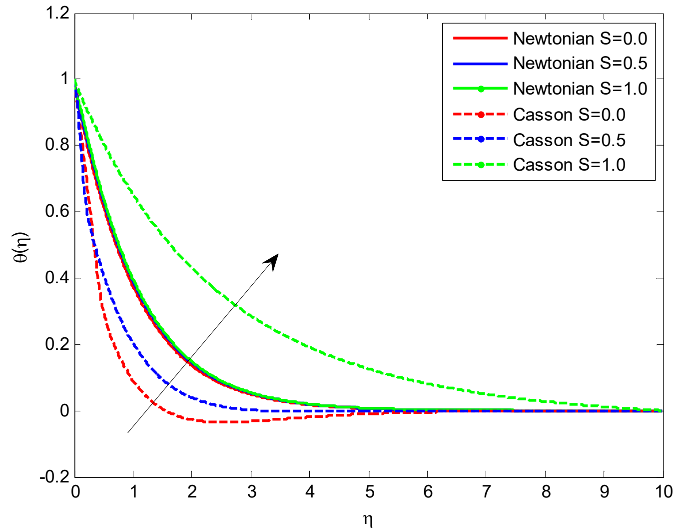

Fig. 21 Effect of S on temperature

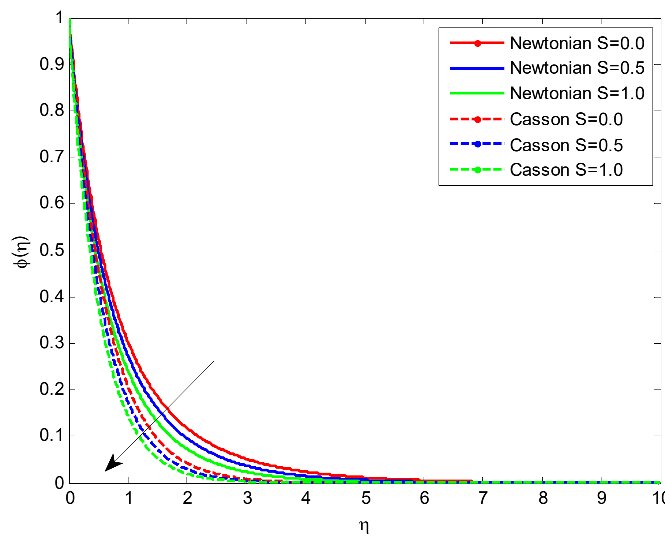

Fig. 22 Effect of S on Concentration

Fig. 2, 3, 4 respectively indicates that with increase in the Hartmann number velocity decreases and temperature, concentration profiles increases due to an opposing force called Lorentz force. It is noticed that temperature plots rise adequately in case of Casson fluid when compared with Newtonian fluid. Fig. 5, 6, 7 respectively indicates that with increase in exponential parameter velocity, temperature and concentration profiles decreases because rise in exponential parameter causes reduction in momentum, thermal and concentration boundary layers. Fig. 8, 9 respectively indicates that with increase in thermal Grashof's number, raise in velocity profiles and decreasing tendency observed in temperature because developing buoyancy force suppress the value of contaminant concentration within the boundary layer regime normal to the barrier. Fig. 10, 11 indicates that with increase in concentration Grashof's number, raise in velocity profiles and fall in concentration profiles is observed. With increase in concentration Grashof's number momentum boundary layer thickness increases concentration boundary layer thickness decreases. Fig. 12 indicates that increase in Radiation parameter temperature enhancement is observed for both fluids. This happens due to the reason that raise in radiation heat energy with that effect temperature increases. Fig. 13 indicates that increase in Prandtl number temperature decreases for both fluids. For Large values of Prandtl number heat spreads slowly from surface when compared to smaller values of Prandtl number. Fig. 14 indicates that increase in heat source parameter temperature diminishes for both the fluids due to decrease in thermal boundary layer thickness. Fig. 15 indicates that enhancement in Eckert number (Ec) raise in thermal conductivity of the fluid is observed so temperature of fluid increases. Fig.16 indicates that with increase in Schmidt number mass transfer increases so concentration profiles decreases. Fig. 17 indicates that increase in chemical reaction parameter, concentration profiles decreases. Fig. 18, 19 indicates that with increase in hall parameter, velocity increases and reverse trend is observed for temperature. Fig.20, 21, 22 indicates that increase in S fluid will come nearer to the surface which causes reduction in thermal, momentum and concentration boundary layer thickness diminishes so velocity and concentration profiles decreases.

To check the validity of the numerical method, results are compared with existing literature by calculating $-f''(0)$ for various values of magnetic field parameter (Hartmann number) by taking
$Gr = Gc = S = 0.0, Rd = 1.0, N = 1.0, \Pr = 0.7,$
$Sc = 0.7, Ec = 0.2, Q = 0.2, G = 0.1, B \to \infty$

Table1 Comparison of $-f''(0)$

Ha	Present study	Ibrahim.et.al (HAM) (2020)	Kameswaran.et.al (RK Fehlberg) (2012)
0.0	1.281814	1.281803	1.281809
1.0	1.629147	1.629170	1.629178

By observing above table excellent correlation is observed with previous results for values of $-f''(0)$. On increasing Hartman number, substantial resistance in flow which causes raise in skin friction values. The influence of various parameters on the skin friction coefficient, Nusselt number, and Sherwood number for the Newtonian and Casson fluids is shown in Tables 2 and 3.

Table 2 Table of parameters skin friction coefficient, Nusselt number, Sherwood number in case of Newtonian fluid

N	Ha	Gr	Gc	S	Pr	R	Q	Ec	Sc	γ	J	m	$(1+\frac{1}{\beta})f''(0)$	$-\left(1+\frac{4R}{3}\right)\theta'(0)$	$-\phi'(0)$
1.5	0	0.1	0.1	0.5	0.7	0.1	0.2	0.2	0.6	0.1	0	0	-1.853711	1.56572	1.449699
	0.3												-1.873202	1.558491	1.445596
	0.8												-2.058748	1.477606	1.421723
1.5	0.5	0.2	0.1	0.5	0.7	0.1	0.2	0.2	0.6	0.1	0	0	-1.816384	1.579024	1.461124
		0.5											-1.565527	1.661807	1.515356
		1											-1.197801	1.762485	1.573135
1.5	0.5	0.1	0.2	0.5	0.7	0.1	0.2	0.2	0.6	0.1	0	0	-1.829514	1.582447	1.456583
			0.5										-1.612301	1.662566	1.501623
			1										-1.280476	1.753283	1.556699
1.5	0.5	0.1	0.1	0	0.7	0.1	0.2	0.2	0.6	0.1	0	0	-1.543743	1.248192	1.336602
				0.6									-1.990505	1.616101	1.460563
				1.2									-2.56068	2.059417	1.610409
1.5	0.5	0.1	0.1	0.5	0.3	0.1	0.2	0.2	0.6	0.1	0	0	-1.903033	0.866205	1.439758
					0.5								-1.905966	1.214185	1.438842
					1								-1.908353	2.026923	1.438156
1.5	0.5	0.1	0.1	0.5	0.7	0	0.2	0.2	0.6	0.1	0	0	-1.907713	1.496123	1.438335
						0.5							-1.905735	1.726055	1.438911
						1							-1.90387	1.931862	1.439489
1.5	0.5	0.1	0.1	0.5	0.7	0.1	0.1	0.2	0.6	0.1	0	0	-1.907028	1.497866	1.438517
							0.5						-1.90814	1.682265	1.438249
							1						-1.90951	1.906957	1.437917
1.5	0.5	0.1	0.1	0.5	0.7	0.1	0.2	0	0.6	0.1	0	0	-1.907395	1.636836	1.438447
								1					-1.906956	1.174491	1.438462
								2					-1.906517	0.712266	1.438477
1.5	0.5	0.1	0.1	0.5	0.7	0.1	0.2	0.2	0.4	0.1	0	0	-1.890318	1.555793	1.095974
									0.8				-1.918081	1.540782	1.705889
									1				-1.927983	1.536984	1.987027
1.5	0.5	0.1	0.1	0.5	0.7	0.1	0.2	0.2	0.6	0	0	0	-1.859435	1.543964	1.55865
										0.5			-1.871946	1.537716	1.707068
										1			-1.880958	1.534623	1.828975
1.5	0.5	0.1	0.1	0.5	0.7	0.1	0.2	0.2	0.6	0.1	0.1	0	-1.86252	1.531867	1.591498
											0.5		-1.862358	1.490644	1.591511
											1		-1.862156	1.439112	1.591526
1.5	0.5	0.1	0.1	0.5	0.7	0.1	0.2	0.2	0.6	0.1	0	0	-1.897509	1.522063	1.584614
												0.5	-1.879693	1.533472	1.588119
												1	-1.852591	1.546542	1.593463

Table-3 Table of parameters skin friction coefficient, Nusselt number, Sherwood number in case of Casson fluid.

N	Ha	Gr	Gc	S	Pr	R	Q	Ec	Sc	γ	J	m	$(1+\frac{1}{\beta})f''(0)$	$-\left(1+\frac{4R}{3}\right)\theta'(0)$	$-\phi'(0)$
1.5	0	0.1	0.1	0.5	0.7	0.1	0.2	0.2	0.6	0.1	0	0	-5.41424	1.853095	1.863675
	0.3												-5.46146	1.849093	1.862614
	0.8												-5.74174	1.824643	1.856298
1.5	0.5	0.2	0.1	0.5	0.7	0.1	0.2	0.2	0.6	0.1	0	0	-5.45567	1.846769	1.862275
		0.5											-5.19489	1.860468	1.866697
		1											-4.77694	1.881268	1.873588
1.5	0.5	0.1	0.2	0.5	0.7	0.1	0.2	0.2	0.6	0.1	0	0	-5.47823	1.844448	1.706777
			0.5										-5.21797	1.858093	1.710093
			0.8										-4.96048	1.871529	1.713391
1.5	0.5	0.1	0.1	0	0.7	0.1	0.2	0.2	0.6	0.1	0	0	-5.21825	1.915135	1.549382
				0.3									-5.63958	1.883	1.738069
				1									-6.11114	2.328931	1.938162
1.5	0.5	0.1	0.1	0.5	0.3	0.1	0.2	0.2	0.6	0.1	0	0	-5.53606	1.169879	1.860854
					0.5								-5.54173	1.525454	1.860779
					1								-5.54661	2.284788	1.860725
1.5	0.5	0.1	0.1	0.5	0.7	0	0.2	0.2	0.6	0.1	0	0	-5.54527	1.749458	1.860739
						0.5							-5.54127	2.184569	1.860784
						1							-5.53765	2.565606	1.860832
1.5	0.5	0.1	0.1	0.5	0.7	0.1	0.1	0.2	0.6	0.1	0	0	-5.54428	1.816144	1.86075
							0.5						-5.5449	1.918948	1.860741
							1						-5.54567	2.045509	1.86073
1.5	0.5	0.1	0.1	0.5	0.7	0.1	0.2	0	0.6	0.1	0	0	-3.55831	1.909817	1.629662
								1					-3.55758	1.187979	1.629666
								2					-3.55684	0.466352	1.62967
1.5	0.5	0.1	0.1	0.5	0.7	0.1	0.2	0.2	0.4	0.1	0	0	-5.51808	1.843645	1.348453
									0.8				-5.5492	1.841755	1.974509
									1				-5.55976	1.841257	2.249723
1.5	0.5	0.1	0.1	0.5	0.7	0.1	0.2	0.2	0.6	0	0	0	-5.53637	1.842327	1.686497
										0.5			-5.54139	1.842242	1.781922
										1			-5.54552	1.842129	1.869108
1.5	0.5	0.1	0.1	0.5	0.7	0.1	0.2	0.2	0.6	0.1	0.1	0	-5.53733	1.823603	1.706317
											0.5		-5.53674	1.748748	1.706326
											1		-5.53601	1.655172	1.706338
1.5	0.5	0.1	0.1	0.5	0.7	0.1	0.2	0.2	0.6	0.1	0	0	-5.664728	1.831206	1.703408
												0.5	-5.614168	1.835648	1.704563
												1	-5.537475	1.842316	1.706314

5. CONCLUSIONS

It is evident from the tables that
1. Raise in the Hartman number reduces the friction factor and the heat and mass transfer rates.
2. Increase in the radiation parameter, thermal Grashof number, and concentration Grashof number increases the skin friction coefficient and the heat and mass transfer rates.
3. The skin friction coefficient declines and the Nusselt number and the Sherwood number grow with increasing suction parameter.
4. As the Prandtl number and the heat source parameter increase, the heat transfer rate grows and the skin friction coefficient and mass transfer rate decrease.
5. Increase in the Eckert number enhances the skin friction coefficient and the mass transfer rate but depreciates the heat transfer rate.
6. As the chemical reaction parameter and Schmidt number rise, the mass transfer rate grows and the skin friction coefficient and the heat transfer rate decrease.
7. Increase in hall parameter, skin friction, heat transfer rate, and mass transfer rate increases.

ACKNOWLEDGEMENTS

The authors are thankful to Koneru Lakshmaiah education Foundation for providing research facilities.

NOMENCLATURE

Ha- Hartman’s number
N- Exponential Parameter
Gr- Thermal Grashof number
Gc- Concentration Grashof number
R- Radiation parameter
Pr- Prandtl number

Ec- Eckert number
Q- Heat generation parameter
Sc- Schmidt number
m- hall parameter
ρ – density of the fluid
k- thermal conductivity of the fluid
k_1- chemical reaction rate
S- Suction parameter

REFERENCES

Anki Reddy, P.B., Suneetha, S., 2018f. "Impact of Catteno-Christov heat flux in the Casson fluid flow over a stretching surface with aligned magnetic field and homogeneous and homogeneous chemical reaction," Frontiers *in Heat and Mass Transfer*, 10. http://dx.doi.org/10.5098/hmt.10.7.

Balamurugan, K. S., Udaya Bhaskara Varma, N., Ramaprasad, J. L., 2020a, "Entropy Generation and Temperature Gradient Heat Source Effects on MHD Couette Flow with Permeable Base in the Presence Of Viscous and Joules Dissipation," *Frontiers in Heat and Mass* Transfer, 15(8). https://doi.org/10.5098/hmt.15.8

Cebeci, T., Bradshaw, P., 1988, "Physical and Computational aspects of Convective Heat Transfer," *springer- verlag*, Newyork. https://doi.org/10.1007/978-1-4612-3918-5

Charan Kumar, G., Jayarami Reddy, K., Ramakrishna, K., Narendradh Reddy, M., 2018e, "Non-uniform heat source/sink and joule heating effects on chemically radiative MHD mixed convective flow of micro polar fluid over a stretching sheet in porous medium," *Defect and Diffusion Forum* , 388, 281-302. https://doi.org/10.4028/www.scientific.net/DDF.388.281

Chandra Sekhar, K.V., 2018c, "Heat transfer analysis of second grade fluid over a stretching sheet through porous medium under the influence of chemical reaction parameter," *International Journal of Mechanical and Production Engineering Research and Development*, 8(1), 605-612. https://doi.org/10.24247/ijmperdfeb201867

Dutta, B.K., Roy, P., Gupta, A.S., (1985), "Temperature field in flow over a stretching sheet with uniform heat flux," *International Communications in Heat and Mass Transfer*, 12(1), 89-94. https://doi.org/10.1016/0735-1933(85)90010-7.

Dharmaiah, G. et al., 2019b, "A Study On Mhd Boundary Layer Flow Rotating Frame Nano fluid With Chemical Reaction," *Frontiers in Heat and Mass Transfer*, 12. http://dx.doi.org/10.5098/hmt.12.10.

Dharmaiah, G., Ali, Chamkha, J., Vedavathi, N., Balamurugan, K.S., 2019o, "Viscous Dissipation Effect on Transient Aligned Magnetic Free Convective Flow Past and Inclined Moving Plate," *Frontiers in Heat and Mass Transfer*, 12, 1-11. https://doi.org/10.5098/hmt.12.17

Dharmaiah, G., Sridhar, W., Balamurugan, K.S., Chandra Kala, K., 2020c, "Hall and ion slip impact on magneto-titanium alloy Nano liquid with diffusion thermo and radiation absorption," *International Journal of Ambient Energy*. https://doi.org/10.1080/01430750.2020.1831597

Flilihi, E., Sriti, M., Achemlal, D., 2019a, "Numerical Solution On Non-Uniform Mesh Of Darcy-Brinkman-Forchheimer Model For Transient Convective Heat Transfer Over Flat Plate In Saturated Porous Medium," Frontiers in Heat and Mass Transfer, 12. http://dx.doi.org/10.5098/hmt.12.12

Ganapathirao, M., Chamkha, A.J., Srinivasa Rao, N., 2019f, "Effects Of Non-Uniform Slot Suction/Injection and Chemical Reaction On Mixed Convective MHD Flow along a Vertical Wedge Embedded In a Porous Medium," *Frontiers in Heat and Mass Transfer*, 13. http://dx.doi.org/10.5098/hmt.13.15

Huang, J., Hsu, H.P., Ay, H., 2019e, "Influence Of Mhd On Free Con vection of Non-Newtonian Fluids over a Vertical Permeable Plate in Porous Media with Internal Heat Generation," *Frontiers in Heat and Mass Transfer*, vol. 13. https://doi.org/10.5098/hmt.13.14

Ibrahim, S.M., Kumar, P.V., Lorenzini, G., 2020e, "Analytical modeling of Heat and Mass Transfer of Radiative MHD Casson Fluid over an exponentially Permeable Stretching Sheet with chemical Reaction," *Journal of Engineering Thermo physics*, 29(1), 136-155. https://doi.org/10.1134/S1810232820010105

James Hartnett, P., Milivoje Kostic 1990a, "Heat Transfer to Newtonian and Non-Newtonian Fluids in Rectangular Ducts," *Advances in Heat Transfer*,19, 247-356. https://doi.org/10.1016/S0065-2717(08)70214-4

Kameswaran, P.K., Narayana, M., Sibanda, P., Makanda, G., 2012, "On radiation effects on hydro magnetic Newtonian liquid flow due to an exponential stretching sheet," *Boundary Value Problems*, 105. https://doi.org/10.1186/1687-2770-2012-105

Khoshrouye Ghiasi, E., Saleh, R., 2018g, "2D Flow of Casson Fluid with Non-Uniform Heat Source/Sink and Joule Heating," *Frontiers in Heat and Mass Transfer*, 12. http://dx.doi.org/10.5098/hmt.12.4.

Konda, J.R., Madhusudhana, N.P., Konijeti, R., 2018d, "MHD mixed convection flow of radiating and chemically reactive Casson Nano fluid over a nonlinear permeable stretching sheet with viscous dissipation and heat source," Multidiscipline Modeling in Materials and Structures, 14(3),609-630. https://doi.org/10.1108/MMMS-10- 2017-0127 .

Kumar, D.R., Reddy, K.J., Raju, M.C., 2019i, "Unsteady MHD thermal diffusive and radiative fluid flow past a vertical porous plate with chemical reaction in slip flow regime," *International Journal of Applied Mechanics and Engineering*, 24(1), 117-129. https://doi.org/10.2478/ijame-2019-0008

Kavitha, P., Naikoti, K., 2019j, "MHD boundary layer flow of non-Newtonian power-law Nano fluid with thermal radiation," *Journal of Nano fluids*, 8(1), 84-93. https://doi.org/10.1166/jon.2019.1567

Kallepalli, N.S., Rajasekhar, K., Ramana Murthy, C.V., 2019k, "Influence of critical parameters on an unsteady state MHD flow in porous channel with exponentially decreasing suction," *Journal of Mathematical and Computational Science*, 9(6), 764-783. https://doi.org/10.28919/jmcs/4249

Lai, F.C., 1990b, "Coupled heat and mass transfer by natural convection from a horizontal line source in saturated porous medium," *International Comm. in Heat and Mass Transfer*, 17(4), 489-499. https://doi.org/10.1016/0735-1933(90)90067-T

Lin, H.T., Wu, C.M., 1995, “Combined heat and mass transfer by laminar natural convection from a vertical plate,” *Heat and Mass Transfer*,30, 369–376.
https://link.springer.com/article/10.1007/BF01647440

Masahide Nakamura., Tadashi Sawada., 1988, “Numerical Study on the Flow of a Non-Newtonian Fluid Through an Axisymmetric Stenosis,”*J Biomech Eng.*110 (2), 1988, 137-143.
https://doi.org/10.1115/1.3108418

Magyari, E., Keller, B., 1999, “Heat and mass transfer in the boundary layers on an exponentially stretching Continuous surface,” *Journal of Physics D: Applied Physics*, Vol. 32(5), 577-585.
https://iopscience.iop.org/0022-3727/32/5/012.

Mukhopadhyay, S., Layek, G.C., Samad, Sk, A., 2005, “Study of MHD boundary layer flow over a heated stretching sheet with variable viscosity,” *International Journal of Heat and Mass Transfer*, 48(21-22),4460-4466.
https://doi.org/10.1016/j.ijheatmasstransfer.2005.05.027

Manjula, V., Chandra Sekhar, K.V., 2019m,” Effect of Soret number and heat source on unsteady MHD Casson fluid flow past an inclined plate embedded in porous medium,” *ARPN Journal of Engineering and Applied Sciences*, 14(11), 2069-2079.

Nagaraju, G., Garvandha, M., Ramana Murthy, J.V., 2019d, “MHD Flow in a Circular Horizontal Pipe under Heat Source/Sink With Suction/ Injection on Wall,” *Frontiers in Heat and Mass Transfer*, 13.
http://dx.doi.org/10.5098/hmt.13.6.

Nagalakshm, P.S.S., Vijaya, N., 2020d, “MHD flow of carreau Nano fluid explored using CNT over a nonlinear stretched sheet,” Frontiers in heat and mass transfer, 14(4), 1-9
https://doi.org/10.5098/hmt.14.4

Reddy, G.V.R., Krishna, Y.H., 2018b, “Soret and dufour effects on MHD micro polar fluid flow over a linearly Stretching sheet, through non-Darcy porous medium,” *International Journal of Applied Mechanics and Engineering*, 23(2), 485-502.
https://doi.org/10.2478/ijame-2018-0028

Raghunandana Sai, E., Ramana Murthy, C.V., 2019h, “Influence of Critical parameters on temperature and velocity for convective flow of a viscous fluid through porous medium,” *International Journal of Innovative Technology and Exploring Engineering*, 8(11 Special Issue 2), 390-394.
https://doi.org/10.35940/ijitee.K1062.09811S219

Subhas Abel, M., Mahantesh, M., Nandeppanavar, Sharanagouda, B., Malipatil., 2010, “Heat transfer in a second grade fluid through a porous medium from a permeable stretching sheet with non-uniform heat source/sink,” *International Journal of Heat and Mass Transfer*, 53(9–10), 1788-1795.
https://doi.org/10.1016/j.ijheatmasstransfer.2010.01.011

Ibrahim, S.M., Suneetha, K., Ramana Reddy, G.V., 2019g, “A study on free convective heat and mass transfer flow through a highly porous medium with radiation, chemical reaction and soret effects,” *Journal Computational and Applied Research in Mechanical Engineering*, 8(2),121-132.
https://doi.org/10.22061/JCARME.2017.2018.1175

Sivaiah, G., Jayarami Reddy, K., Chandra Reddy, P., Raju, M.C., 2019n, “Numerical study of MHD boundary layer flow of a visco elastic and dissipative fluid past a porous plate in the presence of thermal radiation,” *International Journal of Fluid Mechanics Research*, 46(1), 27-38.
https://doi.org/10.1615/InterJFluidMechRes.2018020153

Talla, H., Kumari, P., Sridhar, W., 2018a, “Numerical study to diffusion of chemically reactive species over MHD exponentially stretching surface of a casson fluid,” *International Journal of Mechanical Engineering and Technology*, 9(10), 470- 481.

Vedavathi, N., Ramakrishna, K., Reddy, K.J., 2015, “Radiation and Mass transfer effects on unsteady MHD convective flow past an Infinite vertical plate with Dufour and Soret effects,” *AinShams Engineering Journal*, 6(1), 363-371.
https://doi.org/10.1016/j.asej.2014.09.009

Vedavathi, N., Dharmaiah G., Balamurugan K.S., Prakash J., 2017, “Heat transfer on MHD Nano fluid flow over a semi infinite flat plate embedded in a porous medium with radiation absorption, heat source and diffusion thermo effect,” *Frontiers in Heat and Mass Transfer*, 9(38).
https://doi.org/10.5098/hmt.9.38

Vijaya, K., Reddy, G.V.R., 2019l, “Magneto hydrodynamic Casson fluid flow over a vertical porous plate in the Presence of radiation, Soret and chemical reaction effects,” *Journal of Nano fluids*, 8(6), 1240-1248.
https://doi.org/10.1166/jon.2019.1684

V.S., S.K., Pai, N.P., 2019c, “Suction and injection effect on flow between two plates with reference to Casson fluid model,” Multidiscipline *Modeling in Materials and Structures*, 15(3), 559 –574.
http://dx.doi.org/10.1108/mmms-05-2018-0092.

Vijaya, N., Arifuzzaman, S.M., Sai, N.R., Rao, C.M., 2020b, “Analysis of Arrhenius activation energy in electrically conducting casson fluid flow induced due to permeable elongated sheet with chemical reaction and viscous dissipation,” *Frontiers in heat and mass transfer*, 15(1), 1-9.
https://doi.org/10.5098/hmt.15.26